

On the dynamics of turbulent transport near marginal stability

P. H. Diamond and T. S. Hahm

Citation: *Physics of Plasmas* **2**, 3640 (1995); doi: 10.1063/1.871063

View online: <http://dx.doi.org/10.1063/1.871063>

View Table of Contents: <http://scitation.aip.org/content/aip/journal/pop/2/10?ver=pdfcov>

Published by the [AIP Publishing](#)

Articles you may be interested in

[The dynamics of marginality and self-organized criticality as a paradigm for turbulent transport](#)
Phys. Plasmas **3**, 1858 (1996); 10.1063/1.871681

[On the consistency of Reynolds stress turbulence closures with hydrodynamic stability theory](#)
Phys. Fluids **8**, 781 (1996); 10.1063/1.868861

[Subgrid-scale energy transfer and near-wall turbulence structure](#)
Phys. Fluids **8**, 215 (1996); 10.1063/1.868829

[Anomalous momentum transport from drift wave turbulence](#)
Phys. Fluids B **5**, 3876 (1993); 10.1063/1.860610

[Energy transfer dynamics of dissipative trapped ion convective cell turbulence](#)
Phys. Fluids B **4**, 599 (1992); 10.1063/1.860258



PFEIFFER VACUUM

VACUUM SOLUTIONS FROM A SINGLE SOURCE

Pfeiffer Vacuum stands for innovative and custom vacuum solutions worldwide, technological perfection, competent advice and reliable service.

On the dynamics of turbulent transport near marginal stability

P. H. Diamond^{a)}

Department of Physics, University of California, San Diego, 9500 Gilman Drive, La Jolla, California 92093-0319

T. S. Hahm

Princeton Plasma Physics Laboratory, Princeton University, P.O. Box 451, Princeton, New Jersey 08543

(Received 1 February 1995; accepted 14 June 1995)

A general methodology for describing the dynamics of transport near marginal stability is formulated. Marginal stability is a special case of the more general phenomenon of self-organized criticality. Simple, one field models of the dynamics of tokamak plasma self-organized criticality have been constructed, and include relevant features such as sheared mean flow and transport bifurcations. In such models, slow mode (i.e., large-scale, low-frequency transport events) correlation times determine the behavior of transport dynamics near marginal stability. To illustrate this, impulse response scaling exponents (z) and turbulent diffusivities (D) have been calculated for the minimal (Burgers') and sheared flow models. For the minimal model, $z=1$ (indicating ballistic propagation) and $D\sim(S_0^2)^{1/3}$, where S_0^2 is the noise strength. With an identically structured noise spectrum and flow with shearing rate exceeding the ambient decorrelation rate for the largest-scale transport events, diffusion is recovered with $z=2$ and $D\sim(S_0^2)^{3/5}$. This indicates a qualitative change in the dynamics, as well as a reduction in losses. These results are consistent with recent findings from dimensionless scaling studies. Several tokamak transport experiments are suggested. © 1995 American Institute of Physics.

I. MOTIVATION AND INTRODUCTION

The concept of marginal stability¹ is an oft-used paradigm in tokamak confinement physics. The marginal stability hypothesis is simply the notion that when a local gradient exceeds the critical value set by a stability criterion, the fluctuation-driven flux increases rapidly, and thus drives the gradient back to marginality. As a consequence, energy content (and thus confinement time) is determined by the marginal stability criterion alone, and is not sensitive to the detailed nonlinear evolution of the instability process. Possible applications of the marginal stability construct include the following.

(i) The instance of transport near the β limit, where marginally stable magnetohydrodynamics (MHD) modes (i.e., ballooning modes) and microturbulence jointly regulate confinement. This scenario has been invoked to explain general L-mode confinement scaling, as well.²

(ii) The hypothesis that tokamak core transport is determined by the marginal stability threshold for ion temperature gradient instabilities in the presence of a background of electron drift waves.³⁻⁵

(iii) Edge transport in the H mode, where residual turbulence (reduced, perhaps to marginality, by electric field shear) and neoclassical ion thermal conduction combine to control the edge transport barrier.

All these specific realizations have certain basic constituents in common. These include the following.

(i) A marginally stable profile, which is defined by the threshold criterion (usually linear) for some instability.

(ii) An "ambient" or "background" transport mechanism, which is unrelated to any exceedance of the threshold

condition. In addition, the ambient transport must be weak in comparison to any which results when marginal stability is strongly violated.

(iii) A noise source, which accounts for fluctuations in heating and fueling about the levels (of external drive) necessary for marginality.

(iv) Some assumptions concerning profile boundary conditions.

Taken together, these common constituents effectively define the marginal stability paradigm. The goal of this paper is to characterize the dynamics of transport near marginality and develop the theoretical foundations for predictive modeling of tokamak plasmas near marginal stability. To do so, it is useful to observe that the dynamical models that govern marginal stability phenomena (i.e., the basic fluid or kinetic equations, field theories, etc.) are sometimes scale invariant, or, more frequently, support ranges of "approximate" spatiotemporal scale invariance. A marginally stable system described by a scale invariant dynamical model is an example of a *self-organized criticality* (SOC).⁶⁻⁸ A self-organized criticality is a general phenomenon where instability dynamics tend to select a state or class of states that exhibit features akin to those observed near critical points (i.e., long correlation lengths, soft fluctuation modes, etc.). It is important to stress that in the context of turbulent transport, *the self-organized critical state is not necessarily the linearly marginally stable state*. Indeed, the deviation of the SOC state from the linearly marginal state is a measure of the "tightness" of the marginal stability, which is determined by the ratio of turbulent transport to drive (i.e., heating, etc.). It may be said, then, that *all* realizations of the SOC paradigm involve some sort of "marginal stability," but not all examples of "marginal stability" qualify as a self-organized criticality. The motivation for this distinction is that the key elements in

^{a)}Also at General Atomics, San Diego, California 92186.

the dynamics of a SOC are stable, *large-scale transport events*, referred to as “modes.”⁸ Here a “mode” consists of many (evolved) instabilities. Such modes are excited by noise and weakly damped by ambient transport. As a consequence of scale invariance, the large-scale modes exhibit long correlation times, which diverge at large scale (i.e., $\tau_{ck}^{-1} = k^2 D$). Thus, they make a significant contribution to the fluctuation-driven flux, even when they are only weakly excited. For example, consider the generic case, where

$$\Gamma_T = -D_T \frac{\partial \langle P \rangle}{\partial r},$$

$$D_T = \sum_{k, \omega} \langle \tilde{v}^2 \rangle_{k, \omega} \tau_{c_{k, \omega}}.$$

It is easily seen that if $\tau_{c_{k, \omega}}$ diverges at low k , Γ_T can be large, even if $\langle \tilde{v}^2 \rangle_{k, \omega}$ is modest. Indeed, should τ_{c_k} diverge sufficiently rapidly at low k , Γ_T can develop an infrared divergence. Such infrared divergences of the turbulent transport coefficient due to low- k modes with long correlation times (“slow modes”) are a distinguishing characteristic of an SOC. Obviously, the dynamics of transport in a SOC is quite different from the conventional wisdom of linearly unstable modes and quasilinear diffusion, as *linear instability of the slow modes is not required*. We remark here that the observation of Bohm scaling, for which the system (machine) size apparently controls transport, suggests the approach of infrared catastrophe. Hence, slow modes are likely quite important to transport in tokamaks, where Bohm transport is frequently observed.

Transport in the “confinement zone” of a tokamak is a naturally scale-invariant process, since by definition the “confinement zone” is distinguishable from regions of strong heat and particle deposition, because in the confinement zone, turbulent transport dominates all other local processes (i.e., collisional transport, anomalous heat transfer, etc.). Thus, confinement zone transport dynamics near marginal stability is a realization of a self-organized criticality. The more detailed characteristics of a SOC are displayed as well, since (i) “noise” is present, i.e., Beam Emission Spectroscopy (BES) fluctuation measurements⁹ clearly suggest the presence of large-scale fluctuations; (ii) small-scale fluctuations have long been¹⁰ observed. These drive the background or “ambient” transport process; and (iii) the inverse transfer of cascade of energy to large scales typical of strongly magnetized plasmas naturally couples the noise to the large-scale modes of the system.

Taken in together, these arguments suggest that a broad class of problems pertaining to tokamak transport near marginal stability may be amenable to analysis using methods from the theory of self-organized criticality.

At this point, it is useful to briefly review the SOC theory paradigm. The prototypical realization of SOC is the running sandpile, which supports avalanches when the local slope exceeds the angle of repose. Localized avalanches occur, but net balance with noise excitation (i.e., associated with randomly sprinkling sand on the pile) occurs when the avalanches overlap and discharge sand from the pile, thereby maintaining a globally quasisteady state close to the critical

profile (given by the angle of repose). An avalanche should be thought of as analogous to a transport “event,” not a (linear) instability (i.e., a drift wave, etc.). The avalanche power spectrum is consistent with $1/f$, so that the biggest avalanches occur most infrequently and smaller avalanches most often,⁸ in accord with our expectations for a driven system that is “bubbling” near marginal stability. In addition, large-scale global discharges of the sandpile (termed great events) occur infrequently (i.e., at intervals that exceed a confinement time). The frequency and wave number of the avalanches are related by the “critical exponent”¹¹ z , i.e., such that $\omega = ck^z$, where c is some constant. Indeed, the principal output of the SOC theory is the exponent z , which also characterizes the dynamics of the impulse response of the system. Obviously, $z=2$ indicates a diffusive response, $z=1$ suggests a ballistic response, etc. The theory also predicts an effective turbulent transport coefficient (i.e., renormalized diffusivity), which exhibits a (previously mentioned) infrared divergence.¹² Such a divergence effectively renders the renormalized diffusivity *scale dependent*, i.e., if $\delta x^2 \sim D_T \tau$, $D = D_T(\delta x)$. Such scale dependency underlies the anomalous value of the critical exponent (i.e., $z < 2$, indicating superdiffusive behavior), and represents a significant departure from the quasilinear diffusion paradigm¹³ of transport.

In this paper, the dynamics of tokamak plasma transport events near marginal stability are studied, and a simple model derived from the SOC paradigm is advanced. The form of the basic nonlinear evolution equation for the local deviation of the profile from criticality is derived using simple symmetry concepts.⁸ In its simplest incarnation, this equation reduces to Burgers’ equation. However, we also show that it is possible to formulate alternative model equations, including ones appropriate for describing systems with sheared flow [i.e., due to neutral beam injection (NBI)-driven sheared toroidal rotation]¹⁴ or systems that exhibit a transport bifurcation,^{15,16} which are consistent with the fundamental symmetry constraints. The basic model is then analyzed, with the goal of determining the following.

(a) The critical exponent z , which characterizes the dynamics of the nonlinear response of the plasma transport SOC.

(b) The (scale-dependent) effective turbulent transport coefficient. The analysis is implemented in two different ways, via a one-loop renormalization group¹⁷ (RNG) calculation and using the Direct Interaction Approximation (DIA).¹⁸ Not too surprisingly, the results agree. This agreement is a consequence of the random Galilean invariance of the basic equation and the focus on hydrodynamic (low k , ω) phenomena. These together eliminate coupling coefficient and field amplitude renormalization, leaving only propagator renormalization, an effect that is captured by both the DIA and the one-loop RNG. To elucidate the effect of slow modes on transport, the analysis was then repeated for the relevant case when a sheared flow is present. The sheared flow accelerates the rate of decorrelation of long-wavelength, slow modes,¹⁴ thus greatly reducing the severity of the infrared divergence in the turbulent diffusivity and eliminating its dependence on $k_{x\min}$ altogether. As a consequence, the critical

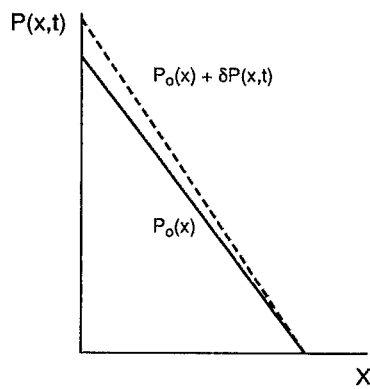


FIG. 1. Depiction of $P_0(x)$ and $P(x,t)$. Note $\delta P(x,t)$ contains information about $P'_0(x)$.

exponent increases from $z=1$ to $z=2$. Moreover, $D_T \sim (S_0^2)^{1/3}$ (S_0^2 is the noise strength) without shear flow, while $D_T \sim (S_0^2)^{3/5}$ with shear flow. The first case exhibits “strong turbulence” scaling, while the latter seems more akin to weak turbulence.

A lengthy discussion of SOC modeling of tokamak transport phenomena follows. This discussion focuses on the following.

(a) Possible experiments (especially transients) to identify and elucidate characteristics of core transport event dynamics that follow from the SOC hypothesis and the implications of this hypothesis for interpreting results.

(b) Ways to exploit the SOC paradigm in transport theory and modeling.

The remainder of this paper is organized in the following manner. In Sec. II, the basic models are derived and discussed. Section III contains the analysis, for both the cases with and without sheared flow. Section IV consists of a summary and a detailed discussion.

II. BASIC DYNAMICAL MODEL

In this section, constraints on the form of a “generic” model for scale invariant dynamics of transport near marginal stability are formulated and discussed. A number of simple models that capture various pieces of the essential underlying physics at large scales are presented. Symmetry properties of the model equations are identified.

The simplest aspect of transport dynamics near marginal stability is the behavior of long-wavelength (large-scale) transport events about a marginally stable profile in one dimension, as shown in Fig. 1, which corresponds to the radial dimension of a tokamak. For concreteness, consider the dynamics of pressure $P(r,t)$ near some marginally stable profile $P_0(r)$. This might correspond to the instance transport near the β limit, for example. Then $\delta p(r,t)$, the deviation of $P(r,t)$ from $P_0(r)$, evolves according to

$$\frac{\partial}{\partial t} \delta P + \frac{\partial}{\partial x} \Gamma[\delta P] - \frac{\partial}{\partial x} D_0 \frac{\partial}{\partial x} \delta P. \quad (1)$$

It is important to again stress that δP should be thought of as a deviation from the mean (i.e., SOC or marginal) profile due

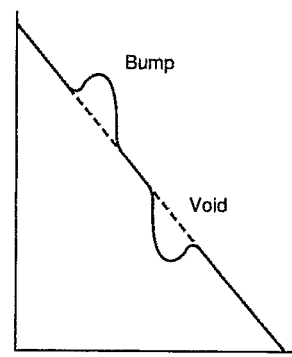
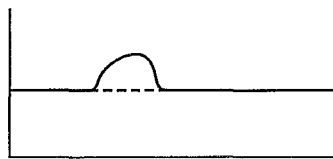


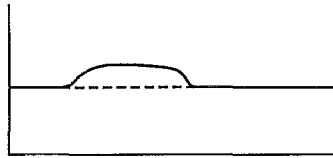
FIG. 2. Depictions of bump and void.

to a transport event, and not as a pressure fluctuation associated with a linear instability. More precisely, a “transport event” will be generated by the interaction of *several* quasi-linear instabilities. Here $\Gamma[\delta P]$ is the flux of pressure, which is, in general, a nonlinear functional of δP . Here D_0 is the ambient or background transport (i.e., as due to drift waves, etc.), so $k^2 D_0 < |\partial \Gamma / \partial x|$, and $\bar{\epsilon}$ is the noise source. Equation (1) states that δP is conserved, up to noise input ($\bar{\epsilon}$) and small-scale dissipation ($k^2 D_0$). The nonlinearity of $\Gamma[\delta P]$ follows from the dependence of the turbulent transport on deviation from marginality. Since $\omega \gg k^2 D_0$, Eq. (1) is approximately scale invariant. The conservative structure of Eq. (1) is crucial for scale invariance. Also, note that $\delta P(x,t) = P(x,t) - P_0(x)$ implicitly contains information about the mean pressure gradient, too.

The nontrivial content of Eq. (1) is, of course, buried in the form of $\Gamma[\delta P]$, which is, in turn, constrained by the presence of a mean gradient $P'_0(r)$ and by the fact that the flux must be down the *total* gradient, locally. Thus, bumps (i.e., localized perturbations with $\delta P > 0$) must travel *down* the mean gradient, while voids (i.e., localized perturbations with $\delta P < 0$) must travel *up* the mean gradient. These conditions are equivalent to the requirement that $\Gamma[\delta P]$ be invariant under the dual transformations $x \rightarrow -x$ and $\delta P \rightarrow -\delta P$. This constraint, first identified by Hwa and Kardar,⁸ is termed joint reflection symmetry. The underpinnings of the joint reflection symmetry constraint are best illustrated pictorially. Figure 2 defines bump and void, respectively. Figures 3(a) and 3(b) show the evolution of a bump in the absence of a mean gradient (i.e., $P'_0 = 0$). Consideration of reflection symmetry reveals that the bump will spread out due to the action of transport. However, the barycenter of the bump remains fixed. Now, consider a bump on a profile with mean $P'_0 < 0$ (Fig. 4). Here, reflection symmetry about the center of the bump is broken, as $P'_0 < 0$. Thus, the piece of the bump enclosed by the curve passing thru points BCD in Fig. 3(a) will propagate *down* the mean gradient (here down the total gradient, as well), while the piece enclosed by the curve passing thru points BAD in Fig. 3(b) will move *up* the mean gradient (but locally *down* the gradient of *total p*!). Since the area enclosed by BCD exceeds the area enclosed by BAD, the net motion of the bump is *down* the mean gradient. A similar pictorial argument reveals that a void must propagate *up* the mean gradient. These simple consid-



(3a)



(3b)

FIG. 3. Time evolution of a symmetric bump.

erations clearly establish the principle of joint reflection symmetry. Note that the requirement of bumps moving “down” and voids moving “up” the local gradient is consistent with non-negative entropy production, as well.

The form of $\Gamma[\delta P]$ must be invariant under $x \rightarrow -x$ and $\delta P \rightarrow -\delta P$. Thus, if

$$\Gamma[\delta P] = \sum_{\substack{n,m \\ q,r}} \left[A_n (\delta P)^n + B_m \left(\frac{\partial}{\partial x} \delta P \right)^m + C_{q,r} \delta P^q \left(\frac{\partial}{\partial x} \delta P \right)^r + \dots \right], \quad (2)$$

then, for odd n , all $A_n = 0$. All m are allowed. However, $C_{q,r} = 0$ for q odd, as well. Noting that $m=1$ simply redefines D_0 , it follows that in the hydrodynamic limit, the *simplest possible form* of $\Gamma[p]$ is $(\lambda/2) \delta P^2$, so that δP evolves according to

$$\frac{\partial}{\partial t} \delta P + \frac{\partial}{\partial x} \left(\frac{\lambda}{2} \delta P^2 \right) - D_0 \frac{\partial^2}{\partial x^2} \delta P = \tilde{s}. \quad (3)$$

Observe that a similar result would follow from the familiar $\Gamma = -D \partial p / \partial x$ [recall $\delta P = p(x,t) - P_0(x,t)$] with $D \sim \delta P$, as typical of fluctuations near marginal stability. However,

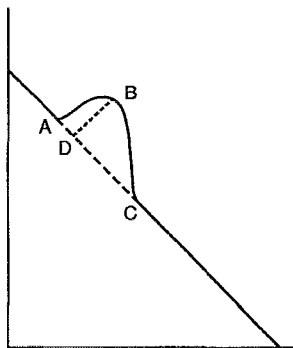


FIG. 4. Net motion of bump is down gradient.

other forms are possible, as well. In particular, a class of forms of $\Gamma[\delta p]$, which allow the possibility of a transport bifurcation^{15,16} above a critical noise level is

$$\Gamma[\delta P] = \frac{\lambda}{2} \frac{\delta P^2}{1 + \alpha \delta P^{2m}}, \quad (4)$$

with m an integer. Here, $\Gamma[\delta P]$ is manifestly invariant under $\delta P \rightarrow -\delta P$, $x \rightarrow -x$ increases as δP^2 for small δP [i.e., as in Eq. (3)], but decreases or remains constant (for $m=1$) with increasing δP (i.e., above a critical noise level) for $\alpha \delta P^{2m} > 1$. This highly nonlinear choice of $\Gamma[\delta P]$ is motivated by the familiar transport bifurcation ansatz $D \rightarrow D_0 / (1 + \alpha E_r'^2)$, and the form of the radial force balance equation. Note also that mean shear flow¹⁴ effects may be introduced into the propagation in two dimensions, via

$$\frac{\partial}{\partial t} \delta P + V_0' x \frac{\partial \delta P}{\partial y} - D_0 \left(\frac{\partial^2}{\partial x^2} + \frac{\partial^2}{\partial y^2} \right) \delta P + \frac{\partial}{\partial x} \left(\frac{\lambda}{2} \delta P^2 \right) = \tilde{s}. \quad (5)$$

Here x is analogous to the radial direction (with mean symmetry about $x=0$) while y is analogous to θ . As $V_0' x$ is invariant under $x \rightarrow -x$, it is clear that Eq. (5) is consistent with joint reflection symmetry. An equation of the form of Eq. (5) may be interpreted as describing marginal stability in a tokamak with sheared toroidal flow or in a long, thin sandpile with a strong sheared wind blowing along its face.

The prototypical model for the long-wavelength transport event dynamics of a system near marginality is that of Eq. (3). This equation is recognized as Burgers' equation for one-dimensional (1-D) hydrodynamics with a random source (i.e., take $\delta P \rightarrow v$). Thus, it is invariant under a random Galilean transformation, as is Burgers' equation.¹⁷ Specifically, the substitution $\delta P(x,t) \rightarrow \delta P_0 + \delta P(x - \lambda \delta P_0 t, t)$, with δP_0 a constant, leaves Eq. (3) unchanged. This invariance is a consequence of the “convective” character of the nonlinearity. Thus, the addition of a sheared flow (in two dimensions), as in Eq. (5), yields a model that is also Galilean invariant. However, the form of $\Gamma[\delta P]$ given in Eq. (4), which supports a transport bifurcation, is *not* Galilean invariant. This suggests that the nonlinear dynamics of a model system with transport bifurcations are likely to be fundamentally different from those of the simplest (Burgers') system. This point will be discussed further in the following section.

III. ANALYSIS

In this section, we analyze the basic models presented in Sec. II. The goal is to determine the critical exponents for the system that characterize the functional form of the (nonlinear) impulse response. The nontrivial exponents and form of response are a consequence of infrared divergence of the turbulent flux (caused by slow modes), which is calculated as well. Such features are not described by the familiar quasilinear paradigm. To elucidate these aspects of the physics and to illustrate the underpinnings of certain technical methods, we first discuss the simple system⁸ [i.e., the minimal Burgers' model of Eq. (3)] of Sec. III A, and proceed to the sheared flow model in Sec. III B.

A. Minimal model

Here, we analyze Eq. (3), the simplest model of a SOC or marginal stability. We seek the critical exponents or, equivalently, the nonlinear “dispersion relation.” We compare three approaches, namely those of simple scaling and symmetry considerations, the familiar direct interaction approximation (DIA), and the dynamic renormalization group (RNG) approach.

Simple scaling yields most of the pertinent and significant results. In particular, if one rescales Eq. (3) according to $x \rightarrow bx, t \rightarrow b^z t$ and $\delta P \rightarrow b^x \delta P$, one obtains

$$\frac{\partial}{\partial t} \delta P - D_0 b^{z-2} \frac{\partial^2}{\partial x^2} \delta P + \frac{\lambda}{2} b^{z+x-1} \frac{\partial}{\partial x} \delta P^2 = \tilde{s} b^{z-x}. \quad (6)$$

A critical issue emerges immediately, namely that random Galilean invariance implies that λ is unrenormalized by nonlinear interaction. This is a consequence of the fact that λ enters the position dependence of δP for the boosted frame [i.e., $\delta P(x, t) \rightarrow \delta P(x - \lambda \delta P_0 t, t)$], which must also be a solution of Eq. (3), which is *scale invariant*. Hence, the only way to reconcile Galilean invariance and scale invariance is to impose the condition that λ be unrenormalized. Thus, $z + x - 1 = 0$. As we are concerned with large-scale, hydrodynamic (i.e., $k \rightarrow 0, \omega \rightarrow 0$) behavior, we require that the *noise* be unchanged by rescaling, i.e., $\lim_{k, \omega \rightarrow 0} \langle \tilde{s}^2 \rangle_{k, \omega}$ must remain invariant after rescaling. Thus (noting dimensions!) $z - x - 1 = 0$. It follows directly that $z = 1$ and $x = 0$. This establishes that the correlation function $\langle \delta P^2(\delta x, \tau) \rangle$ has the form $\langle \delta P^2(\delta x^z / \tau) \rangle$, with $z = 1$. Alternately, $\omega \sim ck^z$ (with $z = 1$ and c a proportionality constant) is revealed to be an effective nonlinear “dispersion relation” for the system. Both position and wave number space representations suggest *ballistic* propagation of perturbations. This is significant, as ordinary quasilinear theory would suggest diffusive propagation [i.e., $\omega = k^2 D, \langle \delta P^2 \rangle = \langle \delta P^2(\delta x^2 / \tau) \rangle$], at a rate set by an anomalous diffusivity. The effective “pulse speed,” namely the proportionality factor between ω and k , must be obtained using approximation methods, such as dimensional analysis, the DIA, or the RNG.

We now seek to identify the cause of the departure from diffusive dynamics and to determine the critical exponents and pulse speed proportionality factor using the familiar direct interaction approximation. Observe that, in this example, symmetry arguments preclude renormalization of λ or δP (analogous to vertex function and wave function renormalization, respectively). Hence, the DIA, which involves only viscosity renormalization (analogous to mass renormalization), contains the features of a general renormalized perturbation theory essential to this application. Specifically, we calculate the renormalized response function. Following standard procedures, the nonlinearity of Eq. (3) is given by

$$N_{k, \omega} = ik\lambda \sum_{k', \omega'} \delta P_{-k'} \delta P_{k+k'}^{(2)}_{\omega+\omega'}, \quad (7a)$$

where

$$\begin{aligned} & [-i(\omega + \omega') + (k + k')^2 D_0] \delta P_{k+k'}^{(2)}_{\omega+\omega'} \\ &= -i\lambda(k + k') \delta P_{k'} \delta P_k. \end{aligned} \quad (7b)$$

The contribution from the second term on the right-hand side (RHS) of Eq. (7b) will vanish upon substitution into Eq. (7a) and integration in the hydrodynamic limit. Thus,

$$N_{k, \omega} = k^2 D \delta P_{k, \omega}, \quad (8a)$$

where, for $k, \omega \rightarrow 0$,

$$D = \lambda^2 \sum_{k', \omega'} |\delta P_{k', \omega'}|^2 \frac{k'^2 D_0}{\omega'^2 + (k'^2 D_0)^2}. \quad (8b)$$

Now, the essence of the DIA is to derive a recursion equation for D , the renormalized diffusivity, by (i) taking $D_0 \rightarrow D$ in Eq. (8b), i.e., the propagator used to solve for $\delta P_{k'+k}^{(2)}$ must be treated self-consistently; and (ii) using the *renormalized* diffusivity to relate $\delta P_{k', \omega'}$ to the noise spectrum in Eq. (8b).

Thus,

$$(-i\omega' + k'^2 D) \delta p_{k', \omega'} = \tilde{s}_{k', \omega'}, \quad (9a)$$

so

$$D = \lambda^2 \sum_{k', \omega'} \frac{|\tilde{s}_{k', \omega'}|^2}{(k'^2 D)^3 [1 + (\omega'/k'^2 D)^2]^2}. \quad (9b)$$

Integrating over ω' , assuming white noise, then yields

$$D = \frac{C_1 \lambda^2 S_0^2}{D^2} \int_{k_{\min}}^{\infty} \frac{dk'}{k'^4}. \quad (10)$$

Here S_0^2 is the mean square noise strength (with dimensions of length/time for dimensionless δP) and $C_1 = \int_{-\infty}^{+\infty} dx' / (1 + x'^2)^2 = \pi/2$, from the ω integral. It follows directly that

$$D = \frac{C_1}{3D^2} \lambda^2 S_0^2 k_{\min}^{-3}, \quad (11a)$$

or, equivalently,

$$D = \left(\frac{C_1}{3} \lambda^2 S_0^2 \right)^{1/3} k_{\min}^{-1}. \quad (11b)$$

Note that D diverges as k_{\min}^{-1} , on account of slow modes. Put another way, the infrared divergence $\sim k_{\min}^{-1}$ obscures the distinction between microscales (characteristic of the scatterers) and macroscales implicit to *any* concept of a transport coefficient. As a consequence, D exhibits an implicit scale dependence $D = D(\delta x)$. Hence, if one considers the microscopic propagation of a pulse according to $\delta x^2 = D\tau$, it follows that $D = (C_1 \lambda^2 S_0^2 / 3)^{1/3} k_m^{-1} \equiv (C_1 \lambda^2 S_0^2 / 3)^{1/3} \times [\delta x^2]^{1/2}$, so then $\delta x^2 \sim (C_1 \lambda^2 S_0^2 / 3)^{2/3} \tau^2$. Thus, the critical exponent is revealed to be $z = 1$, indicating *ballistic response* at the velocity $(C_1 \lambda^2 S_0^2 / 3)^{1/3}$. Observe that the infrared divergence of D due to slow modes underlies the departure from quasilinear intuition.

An alternative approach for calculating z is to use the dynamical RNG. This method utilizes scale transformation recursion equations, constructed using perturbation theory, to calculate renormalized transport coefficients. Here lowest-

order (i.e., third-order) perturbation theory yields a “turbulent diffusivity” in the form of one summation over the “background” mode spectrum. This is, of course, equivalent to a summation over Feynman graphs containing one closed loop (computed by one integration over an internal momentum).¹⁹ From Eqs. (8a) and (8b), it follows that, to one loop,

$$D = D_0 + \lambda^2 \sum_{k', \omega'} |\delta P_{k', \omega'}|^2 \frac{k'^2 D_0}{\omega'^2 + (k'^2 D_0)^2}, \quad (12a)$$

or, upon integrating (assuming white noise),

$$D = D_0 \left(1 + \frac{C_1 \lambda^2 S_0^2}{3 D_0^3} k_{\min}^{-3} \right). \quad (12b)$$

At this point, it is convenient to define the (bare) interaction parameter, $U_I^{(0)} = C_1 \lambda^2 S_0^2 / D_0^3$, so $D_T = D_0 (1 + U_I^{(0)} / 3 k_{\min}^3)$. Observe that $U_I^{(0)} / k_{\min}^3$ is analogous to a “Reynolds number” for this system. Then, noting from the scaling of Eq. (6) that $D_0 \sim b^{z-2}$, it follows that the rescaling recursion equation for D_T is (for $bl_0 = k^{-1}$, so that b is the dimensionless scale parameter):

$$b \frac{\partial}{\partial b} D_T = D_0 b \frac{\partial}{\partial b} \left[b^{z-2} \left(1 + \frac{U_I^{(0)}}{3} (bl_0)^3 \right) \right], \quad (13a)$$

or, to lowest order in $U_I^{(0)}$,

$$b \frac{\partial}{\partial b} D_T = D_T [z - 2 + U_I^{(0)} (bl_0)^3]. \quad (13b)$$

Similarly, a recursion equation for U_I , the *renormalized* interaction parameter (as distinct from $U_I^{(0)}$, the bare parameter) may be derived, noting $U_I = U_I(D_T, \lambda, S_0^2)$. As λ and S_0^2 are unrenormalized, it follows directly that, in the one loop approximation,

$$\frac{\partial}{\partial l} U_I = \frac{-3}{D_T} \left(\frac{\partial D_T}{\partial l} \right) U_I. \quad (14)$$

Here $b \partial / \partial b = \partial / \partial l$, where l is dimensionless (unlike l_0). Now, noting that for $(bl_0)^3 U_I^{(0)} \rightarrow U_I$ and $z = 1$, Eq. (13b) becomes equivalent to

$$\frac{\partial}{\partial l} D_T = (-1 + U_I) D_T. \quad (15)$$

Thus, it is now possible to eliminate D_T from Eq. (14) for U_I , and obtain

$$\frac{\partial}{\partial l} U_I = 3(1 - U_I) U_I. \quad (16)$$

Equation (16), a nonlinear recursion equation for U_I , is the principal result of the RNG analysis. It is straightforward to solve, and working to lowest order in U_I gives

$$U_I = (l' e^l)^3 / 1 + (l' e^l)^3. \quad (17)$$

Finally, recalling that $U_I = U_I^{(0)} (l' e^l)^3 = C_1 \lambda^2 S_0^2 (l' e^l)^3 / D_T^3$ (i.e., note that U_I is defined with the *renormalized* diffusivity), we find the result

$$D_T = (C \lambda^2 S_0^2)^{1/3} [1 + (l' e^l)^3]^{1/3}. \quad (18)$$

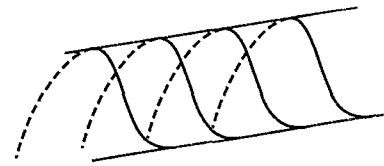


FIG. 5. Depiction of a sandbar.

Here l is the normalized scale ratio. As we expect a result with the generic scaling form $D_T = D_0 (1 + \alpha [\delta x^2]^{\beta/2})^\gamma$, it follows that

$$D_T = D_0 \left(1 + \frac{C_1 \lambda^2 S_0^2}{3 D_0^3} [\delta x^2]^{3/2} \right)^{1/3}, \quad (19)$$

i.e., $\alpha = C_1 \lambda^2 S_0^2 / D_0^3$, $\gamma = \frac{1}{3}$, $\beta = 3$. Note that for $U_I^0 > 1$ (the regime of interest), $D_T \approx (C_1 \lambda^2 S_0^2 / 3)^{1/3} [\delta x^2]^{1/2}$, in agreement with the DIA result of Eq. (11). The scaling $D_T \sim (S_0^2)^{1/3}$ is suggestive of “strong” turbulence. Of course, having deduced that $z = 1$ via similarity arguments, one could obtain the value of α directly from simple dimensional analysis by observing that $U_I^{(0)} / k_{\min}^3 \sim (D_T / D_0)^3 \sim R_e^3$, where R_e is an effective “Reynolds number” for the system. Hence, the principal benefit of an approach via RNG is the construction of a foundation for systematic application to more complex problems, such as those related to transport bifurcations, involving coupling coefficient and wave-function renormalization.

B. SOC in sheared mean flow

We now focus on the dynamics of a SOC in a sheared mean flow. One concrete realization of this paradigm is a long thin sandpile or sandbar, with a sheared wind blowing along its face, as shown in Fig. 5. Another is a tokamak plasma near the β limit, executing differential toroidal rotation. The motivation for devoting such attention to this paradigm is that it highlights the importance of large-scale, slow modes to SOC behavior. We emphasize at the outset that the impact of the sheared flow is not related to its effect on the marginality condition (i.e., the linear instability criterion), which is unchanged. As in Sec. III A, we calculate the critical exponent z and determine the fluctuation-driven flux.

Equation (5) contains the basic description of sandbar dynamics in a sheared wind. Here, x is the distance across the pile, assumed to be symmetric about its center at $x = 0$, and y is the distance along the sandbar (see Fig. 6). For simplicity, $V_y = V_0^l x$. We further assume *radially extended*

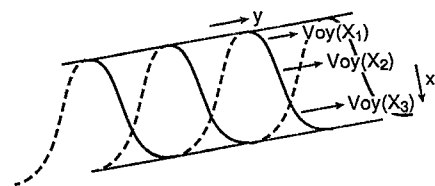


FIG. 6. Depiction of a sandbar in a sheared wind.

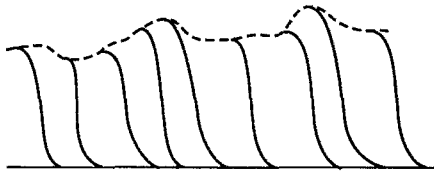


FIG. 7. Sandbar with perturbations due to large-scale noise.

noise. By this we mean that $\langle \tilde{s}^2(k_x, k_y) \rangle$ contains large radial scales, comparable in magnitude to that of the sandbar width. Such noise on large radial scales corresponds to “shaking” the sandbar. With $k_y > k_{y \min}$, such “shaking” is equivalent to random displacement of spanwise uniform slices of the sandbar. Noise with this structure may alternatively be thought of as shaking a loaf of thin-sliced bread, with slices displaced perpendicularly to the loaf’s axis (Fig. 7). Radially extended noise is clearly a “worst case” limit from the standpoint of confinement. This is because radially extended noise eliminates the need for avalanche (or eddy) overlap, in order that sand be ejected from the sandbar. We also remark that radially extended perturbations, with $k_y > k_x$, have a structure similar to twisted slicing modes²⁰ in confined plasmas.

For the case of radially extended noise, the nonlinear term in Eq. (5) may be written as

$$N_{\mathbf{k}, \omega} = ik_x \frac{\lambda}{2} \sum_{\mathbf{k}', \omega'} \delta P_{-\mathbf{k}', -\omega'} \delta P_{\mathbf{k}'+\mathbf{k}, \omega'+\omega}^{(2)}. \quad (20)$$

Here $\mathbf{k} = (k_x, k_y)$, as the perturbations are two dimensional in structure. Proceeding as in standard renormalized perturbation theory (i.e., the DIA),

$$\begin{aligned} & \left(-i(\omega + \omega') + (k_y + k'_y)V_0 \frac{\partial}{\partial k'_x} + \mathbf{k}^{\prime 2} D_0 \right. \\ & \left. + (k_x + k'_x)^2 D_T \right) P_{\mathbf{k}'+\mathbf{k}, \omega'+\omega}^{(2)} \\ & = \frac{-\lambda}{2} (\delta P_{\mathbf{k}', \omega'} ik_x \delta P_{\mathbf{k}, \omega} + ik'_x \delta P_{\mathbf{k}', \omega'} \delta P_{\mathbf{k}, \omega}), \end{aligned} \quad (21a)$$

which, in the hydrodynamic limit, reduces to

$$\begin{aligned} & \left(-i\omega' + k'_y V_0 \frac{\partial}{\partial k'_x} + \mathbf{k}^{\prime 2} D_0 + k_x'^2 D_T \right) \delta P_{\mathbf{k}'+\mathbf{k}, \omega'+\omega}^{(2)} \\ & = \frac{-\lambda}{2} (\delta P_{\mathbf{k}', \omega'} ik_x \delta P_{\mathbf{k}, \omega} + ik'_x \delta P_{\mathbf{k}', \omega'} \delta P_{\mathbf{k}, \omega}). \end{aligned} \quad (21b)$$

Now, the crux of the issue is, of course, what, precisely, is the turbulent decorrelation rate controlling the left-hand side (LHS) of Eq. (21b). There are three possibilities, namely the “collisional” scattering rate $\mathbf{k}^{\prime 2} D_0$, the turbulent radial scattering rate $k_x'^2 D_T$, and the turbulent shear decorrelation rate $(k_y'^2 V_0^2 D_T)^{1/3}$, produced by the synergism of shearing and radially scattering.¹⁴ As $k'_x \sim k'_y$ and $D_T > D_0$, the collisional scattering rate may be immediately discarded. The relative importance of turbulent radial scattering and shear decorrelation is determined by comparing $k'_y V_0 / k'_x$ (from $k'_y V_0 \partial / \partial k'_x$) with $k_x'^2 D_T$, as in the shear suppression¹⁴ crite-

on comparison. Here, anticipating that transport will be dominated by slow, large scales (i.e., in the case of infrared divergence), the comparison at the maximum scale is relevant. Hence, if $k_{x \min}^{\prime 2} D_T > (k'_y V_0 / k'_x)_{\min}$, the slow mode correlation time is given by $(k_{x \min}^{\prime 2} D_T)^{-1}$, as before. If $(k'_y V_0 / k'_x)_{\min} > k_{x \min}^{\prime 2} D_T$, then $1/\tau_{c\mathbf{k}'} = (k_{y \min}^{\prime 2} V_0^2 D_T)^{1/3}$. For the case where shear decorrelation is dominant,

$$N_{\omega}^{\mathbf{k}} = \frac{-\partial}{\partial x} D_T \frac{\partial}{\partial x} \delta P_{\mathbf{k}, \omega} \quad (22a)$$

where

$$D_T = \frac{\lambda^2}{4} \sum_{\mathbf{k}', \omega'} |\delta P_{\mathbf{k}', \omega'}|^2 R_{\mathbf{k}', \omega'} \quad (22b)$$

is the (Markovian) turbulent diffusivity and $R_{\mathbf{k}', \omega'}$ is the resonance function,

$$R_{\mathbf{k}', \omega'} = \frac{1/\tau_{c\mathbf{k}'}}{(\omega' - k'_y V_0 x)^2 + 1/\tau_{c\mathbf{k}'}} \quad (22c)$$

with $1/\tau_{c\mathbf{k}'} = (k_y'^2 V_0^2 D_T)^{1/3}$. In deriving Eq. (22), it is useful to note that $\sum_{\mathbf{k}', \omega'} \delta P_{-\mathbf{k}', -\omega'} k'_x \delta P_{\mathbf{k}', \omega'} R_{\mathbf{k}', \omega'} \rightarrow 0$, by symmetry. Note that here, $\tau_{c\mathbf{k}', \omega'}$ is determined by shear decorrelation. Since $R_{\mathbf{k}', \omega'}$ is treated self-consistently, D_T (not D_0) appears in the shear decorrelation rate. Assuming “white noise” in \mathbf{k} yields (upon substitution for $\delta P_{\mathbf{k}', \omega'}$),

$$D_T = \lambda^2 S_0^2 \sum_{\mathbf{k}', \omega'} \frac{(k_y'^2 V_0^2 D_T)^{1/3}}{[(\omega' - k'_y V_0 x)^2 + (k_y'^2 V_0^2 D_T)^{2/3}]^2}. \quad (23)$$

Observe that the trivial k'_x integral has been absorbed into S_0^2 as a normalization factor. Note also that the noise spectrum need only be white at large scales, as diffusive decorrelation ($k_x'^2 D_T$) will surpass any contribution from small scales. The crucial point is, of course, that now $(k_y'^2 V_0^2 D_T)^{1/3}$ determines the decorrelation rate for the slow modes. This decorrelation rate exhibits *much* weaker \mathbf{k}' scaling than the diffusive decorrelation rate does. Performing the ω' integration gives

$$D_T = C_1 \frac{S_0^2 \lambda^2}{4} \frac{\int_{k_{y \min}}^{\infty} dk'_y}{(k_y'^2 D_T V_0^2)^{2/3}} \quad (24a)$$

or

$$D_T = C_1' \frac{S_0^2 \lambda^2}{(D_T V_0^2)^{2/3}} k_{y \min}^{-1/3}, \quad (24b)$$

where $C_1' = 3C_1/4$. Thus, we finally find

$$D_T = \frac{(C_1' S_0^2 \lambda^2)^{3/5}}{(V_0')^{4/5}} k_{y \min}^{-1/5}. \quad (25)$$

Here D_T is infrared divergent, but *much less severely*, so then in the case $V_0' = 0$ [i.e., compare Eq. (20) with Eq. (11b)]. Note also that D_T is *independent* of $k_{x \min}$! This is an *ab initio* consequence of the fact that shear decorrelation controls the slow mode dynamics, because of the weaker infrared divergence of the shear decorrelation time [$\tau_c \sim (k_y'^2 V_0^2 D_T)^{-1/3}$] than the diffusive decorrelation time

$[\tau_c \sim (k_x^2 D_T)^{-1}]$. Shearing thus “speeds up” the decorrelation of slow modes, so they do not contribute as heavily to transport. Thus, $D_T \sim k_y^{-1/5}$, rather than $D_T \sim k_x^{-1}$, as in Eq. (11b). Finally, we caution the reader that taking the limit $(k_y V_0' / k_x')_{\min} > k_x'^2 D_T$ early in the calculation for simplicity precludes a result that may be extrapolated directly to $V_0' = 0$.

To obtain the critical exponent, it is useful to note that D_T is independent of k_x , so that $D_T \sim D_T([\delta x^2]^0)$. As a result, $\delta x^2 \sim D_T \tau$, so that $z=2$. *Diffusive propagation is thus restored when $(k_y V_0' / k_x')_{\min} > k_x'^2 D_T$* . Moreover, in this regime $D_T \sim (S_0^2)^{3/5}$, suggestive of a “weaker” turbulence scaling. Thus, we arrive at the central result of this section, which is the observation that a strongly sheared wind *raises* the critical exponent for a SOC sandbar from the ballistic limit value $z=1$ to the diffusive value $z=2$. This represents a *qualitative* change in the transport dynamics, not just a decrease in the magnitude of the diffusivity. Note that the cross-stream noise structure is the same in both cases and that the sheared wind does not affect the marginality condition. Hence, the observed trend toward diffusive dynamics can only be ascribed to the acceleration of slow modes by shear decorrelation. It is important to recall that k_y and k_x are the wave numbers of “transport events” (as opposed to linear modes) and that the shear suppression criterion need apply only in the infrared limit (i.e., to slow modes), not throughout the spectrum. It suggests that shearing, via its effect on the infrared behavior of the correlation time, may alter the observable, qualitative *macroscopic* hydrodynamic response of SOCs, such as sandbars in a sheared wind or differentially rotating tokamak plasmas, to invariant noise spectra. Finally, note this argument does *not* rely on turbulence amplitude suppression!

IV. DISCUSSION AND CONCLUSION

In this paper we have formulated and presented a general methodology for describing the dynamics of transport near marginal stability. In particular, the scaling exponents of the impulse response have been identified as quantitative indicators of the dynamical behavior of the marginal system. In turn, the relationship of the observable scaling exponents to the infrared structure of the turbulent transport theory has been established. The principal results of this paper are summarized below.

(a) Simple, one field, one-dimensional models of marginal SOCs have been formulated. The structure of these models is constrained by the requirement of joint reflection symmetry. The minimal version of the SOC model reduces to the familiar Burgers’ equation form, and alternative, more complex, models incorporating sheared mean flow and transport bifurcations have been derived.

(b) The renormalized diffusivity and impulse response scaling exponents have been calculated. Galilean invariance and interest in hydrodynamic behavior eliminate coupling coefficient and wave function renormalization in the case of the minimal (Burgers’) model. As a result, only diffusivity renormalization survives, so the DIA and RNG methods yield identical results. However, coupling coefficient and

wave-function renormalization must be treated in the analyses of more complex models, such as those involving transport bifurcations.

(c) Scaling exponents for the minimal (i.e., Burgers’) and sheared flow model have been calculated. For the minimal model $z=1$, indicating a ballistic response. Moreover, $D_T \sim (S_0^2)^{1/3}$, as in strong turbulence. For shear flow (with $(k_y V_0' / k_x')_{\min} > k_x'^2 D_T$, $z=2$, indicating diffusive response. The values of the scaling exponents are set by the degree of infrared divergence of the turbulent transport coefficient. Thus, since without shear flow, $D_T \sim k_x^{-1}$, $z=1$. With shear flow (but for identical noise) $D_T \sim k_y^{-1/5} k_x^0$, so $z=2$. Here, $D_T \sim (S_0^2)^{3/5}$, indicating “weaker” turbulence. Note that the dominance of shearing results in a *qualitative* change in transport dynamics, not just a reduction in diffusion. This contrast suggests that the scaling of the slow mode correlation time determines the qualitative features of the macroscopic dynamics of transport in a SOC. It also suggests that the long-wavelength correlation times of *stable*, large-scale modes are crucial to predicting transport.

These results have interesting implications for experiment, interpretation, and theory. First, they strongly suggest that impulse response scaling exponents be measured using electron cyclotron resonance heating (ECH) heat pulse propagation experiments.²¹ Previously, attention has been focused on the pulse propagation rate,²² rather than on spatiotemporal evolution (i.e., *shape*). The latter is obviously of much greater utility to the characterization of marginal stability states in tokamaks. Moreover, certain pulse propagation comparisons naturally suggest themselves. These include the following:

(a) Comparing a neo-Alcator Ohmic discharge (likely below marginality) to a balanced injection L-mode discharge that is expected to be marginal to ion temperature gradient (ITG) instability and to a discharge near the β limit, where the marginality is tighter.

(b) Comparing an L-mode plasma to a Very High (VH)-mode plasma,²³ where strong shearing should accelerate the decorrelation of slow modes. In this case, one might expect a trend from $z=1$ in the former to $z=2$ in the latter.

(c) Comparing a case of balanced, on-axis NBI to a case combining on-axis coinjection with off-axis counterinjection, to maximize the toroidal velocity *shear*. Here one could quantitatively test whether the predicted restoration of diffusive dynamics (i.e., $z=1 \rightarrow z=2$) is satisfied.

It would be most amusing to complement these pulse propagation studies by fluctuation measurements. This would yield insight into the relative importance of changes in decorrelation rate and fluctuation amplitude. In particular, the relative change in transport could easily exceed the relative change in fluctuation levels. Most importantly, the observation of anomalous exponents (i.e., $z < 2$) would be a clear-cut indication of marginal stability controlling the dynamics.

A second application of the results is to the realm of interpretation. Here, we note that recently, a great deal of attention has been focused on ρ_* -scaling experiments,²⁴ with the aim of distinguishing gyro-Bohm transport from Bohm transport. Noting that Bohm transport implies that the system size significantly impacts the transport mechanism, it is ap-

parent that Bohm scaling must be indicative of a trend toward an infrared catastrophe. Moreover, the recent observation that ρ_* scaling changes from Bohm in the L mode to gyro-Bohm in the H mode²⁵ suggest that infrared catastrophe in the former ($z=1$) is healed in the latter ($z=2$), presumably by the effect increased electric field shear on large-scale transport events. Our findings concerning the effects of changing slow mode decorrelation rates are consistent with these results. Hence, it would be quite interesting to complement ρ_* -scaling scans with measurements of the pulse-shape scaling exponent.

A third realm of application is to transport theory. First, the SOC theory should be extended to three dimensions and to the model where transport bifurcations can occur. In this case, the SOC is expected to heal itself at sufficient noise levels, i.e., $\partial\Gamma/\partial(S_0^2)$ should change sign at a critical noise level. The evolution of scaling exponents through the bifurcation, as well as the sensitivity of the bifurcation to the structure of the noise are worthy of investigation, too. Note that the analytical theory of the transport bifurcation SOC is much more challenging than the simple noisy Burgers' model, since Galilean invariance is broken. Hence, coupling coefficient and wave-function renormalization are required. This is not surprising, since one way of looking at a transport bifurcation in a 1-D SOC is as an amplitude-dependent coupling, where $\lambda \rightarrow \lambda/(1 + \alpha \delta P^{2m})$. Here, for $S_0^2 > S_{0,crit}^2$, one should expect the Burgers' shocks to smooth out and weaken.

Another implication (for theory) of this work is that the nonlinear dynamics of slow, large-scale modes in the presence of noise is critical to transport, even if such modes are, in fact, not unstable or even weakly damped. This suggests that trapped ion turbulence, with self-consistent evolution of a radial electric field shear, be studied in the presence of general, short-wavelength, noise excitation. The importance of this problem is supported by the ubiquitous finding of Bohm diffusion, in the L mode as well.

The concept of a dynamic marginal stability has implications for transport modeling, as well. For example, if, in fact, the tokamak core is ion temperature gradient (ITG) mode marginal, transient experiments can be simulated using a simple model similar to the ones discussed here. The parameters D_0 , λ , etc., could be determined by scaling arguments or by empiricism. Enormous savings in analysis and computer time would result, and insight would be furthered.

A final, theoretical point is worthy of some additional discussion. The principal new calculation presented in this paper is that which predicts the superdiffusive scaling exponent $z=1$. An alternative approach²⁶ to that problem was previously advanced in Ref. 26, by Lazzara and Putterman. In that work, it was suggested that superdiffusive scaling was linked to the radial propagation of turbulence envelope modulation waves. Such waves resemble second sound, i.e., oscillations in the gas of phonons, or, in the case of a tokamak plasma, "drift-ons." A complete and accurate assessment of this interesting suggestion, however, requires analysis of such drift-on envelope modes in the context of a realistic model of drift wave turbulence in a torus, including Landau resonance dissipation, etc. In the theory presented

here, superdiffusive scaling appeared as a natural consequence of weakly damped, long-wavelength "transport" modes (called slow modes) that do not propagate radially. The envelope of such waves loosely corresponds to "second sound," but here, all perturbations are locally damped at sufficiently long times. From a theoretical perspective, second sound emerges from modulational oscillations in the gas of phonons, while here the noise spectrum is prescribed and fixed. One could also envision calculating the feedback of ballistically propagating transport modes on short-wavelength drift wave turbulence as part of an improved subgrid scale model for transport, which would combine aspects of the modulational wave and scale-dependent diffusivity calculations.

ACKNOWLEDGMENTS

We acknowledge stimulating discussions with and interest from Terence Hwa, B. A. Carreras, A. V. Gruzinov, V. B. Lebedev, and G. I. Soloviev. T.-S. Hahm would like to thank K. H. Chung and S. H. Hong of Seoul National University, where part of this work was performed.

This work was supported by the U.S. Department of Energy under Grant No. DE-FG03-88ER53275 and Contract No. DE-AG02-76-CHO-3073.

- ¹W. M. Manheimer and T. M. Antonsen, *Phys. Fluids* **22**, 957 (1979).
- ²J. W. Connor, J. B. Taylor, and M. Turner, *Nucl. Fusion* **22**, 256 (1984).
- ³T. S. Hahm and W. M. Tang, *Phys. Fluids B* **1**, 1185 (1989).
- ⁴H. Biglari, P. H. Diamond, and M. N. Rosenbluth, *Phys. Fluids B* **1**, 109 (1989).
- ⁵M. Kotschenreuther, W. Dorland, M. Beer, and G. Hammett, *Phys. Plasmas*, **2**, 2381 (1995).
- ⁶P. Bak, C. Tang, and K. Wiesenfeld, *Phys. Rev. Lett.* **59**, 381 (1987).
- ⁷J. Carlson and J. S. Langer, *Phys. Rev. Lett.* **62**, 2632 (1989).
- ⁸T. Hwa and M. Kardar, *Phys. Rev. A* **45**, 7002 (1992).
- ⁹R. Fonck, R. Durst, H. Evensen, J. S. Kim, N. Bretz, E. Mazzucato, R. Nazikian, S. F. Paul, W. W. Lee, F. Levinton, S. E. Parker, R. Santoro, S. Scott, W. Tang, G. Taylor, M. Zarnstorff, the TFTR Group, A. C. England, G. R. Hanson, M. Murakami, and J. B. Wilgen, "Plasma turbulence and associated transport in TFTR D-D and D-T discharges," in *Proceedings of the 15th International Conference On Plasma Physics and Controlled Nuclear Fusion Research*, Seville, Spain, 1994 (International Atomic Energy Agency, Vienna, 1995), Paper A2-4-P-7.
- ¹⁰A. J. Wootton, B. A. Carreras, H. Matsumoto, K. McGuire, W. A. Peebles, Ch. P. Ritz, P. W. Terry, and S. J. Zweben, *Phys. Fluids B* **2**, 2879 (1990).
- ¹¹N. Goldenfeld, *Lectures on Phase Transitions and the Renormalization Group* (Addison-Wesley, Reading, MA, 1992).
- ¹²P. C. Hohenberg and B. I. Halperin, *Rev. Mod. Phys.* **49**, 435 (1977).
- ¹³R. Z. Sagdeev and A. A. Galeev, *Nonlinear Plasma Theory* (Benjamin, New York, 1969).
- ¹⁴H. Biglari, P. H. Diamond, and P. W. Terry, *Phys. Fluids B* **2**, 1 (1990).
- ¹⁵F. L. Hinton, *Phys. Fluids B* **3**, 696 (1991).
- ¹⁶P. H. Diamond, Y. M. Liang, B. A. Carreras, and P. W. Terry, *Phys. Rev. Lett.* **72**, 2565 (1994).
- ¹⁷D. Forster, D. R. Nelson, and M. J. Stephen, *Phys. Rev. A* **16**, 732 (1977).
- ¹⁸R. H. Kraichnan, *J. Fluid Mech.* **5**, 497 (1959).
- ¹⁹H. W. Wyld, *Ann. Phys. NY* **14**, 143 (1961).
- ²⁰K. V. Roberts and J. B. Taylor, *Phys. Fluids* **8**, 315 (1965).
- ²¹T. C. Luce, C. C. Petty, and J. C. M. De Haas, *Phys. Rev. Lett.* **68**, 52 (1992).
- ²²J. P. Christiansen, P. M. Stubberfield, J. G. Cordey, and C. Gormezano, *Nucl. Fusion* **33**, 863 (1993).
- ²³K. H. Burrell, *Plasma Phys. Controlled Fusion* **36**, 291 (1994).

²⁴F. W. Perkins, C. W. Barnes, D. W. Johnson, S. D. Scott, M. C. Zarnstorff, M. G. Bell, R. E. Bell, C. E. Bushj, B. Grek, K. W. Hill, D. K. Mansfield, H. Park, A. T. Ramsey, J. Schivell, B. C. Stratton, and E. Synakowski, *Phys. Fluids B* **5**, 477 (1993).

²⁵T. C. Luce, C. C. Petty, K. H. Burrell, C. B. Forest, P. Gohil, R. J. Groebner, J. C. M. DeHaas, R. A. James, and M. A. Makowski, "Experimental constraints on transport," in Ref. 9, Paper No. A2-111-2.

²⁶A. Lazzara and S. Putterman, *Phys. Rev. Lett.* **57**, 2810 (1986).